

Exploring the effects of geotextiles in the performance of highway filter drains for sustainable and resilient highway drainage

Sanudo-Fontaneda, L., Coupe, S., Charlesworth, S. & Rowlands, E. G.

Author post-print (accepted) deposited by Coventry University's Repository

Original citation & hyperlink:

Sanudo-Fontaneda, L, Coupe, S, Charlesworth, S & Rowlands, EG 2018, 'Exploring the effects of geotextiles in the performance of highway filter drains for sustainable and resilient highway drainage' *Geotextiles & Geomembranes*, vol. 46, pp. 559-565.

<https://dx.doi.org/10.1016/j.geotexmem.2018.04.006>

DOI 10.1016/j.geotexmem.2018.04.006

ISSN 0266-1144

Publisher: Elsevier

NOTICE: this is the author's version of a work that was accepted for publication in *Geotextiles and Geomembranes*. Changes resulting from the publishing process, such as peer review, editing, corrections, structural formatting, and other quality control mechanisms may not be reflected in this document. Changes may have been made to this work since it was submitted for publication. A definitive version was subsequently published in [*Geotextiles and Geomembranes*, [46], (2018) DOI: 10.1016/j.geotexmem.2018.04.006

© 2017, Elsevier. Licensed under the Creative Commons Attribution-NonCommercial-NoDerivatives 4.0 International

<http://creativecommons.org/licenses/by-nc-nd/4.0/>

Copyright © and Moral Rights are retained by the author(s) and/ or other copyright owners. A copy can be downloaded for personal non-commercial research or study, without prior permission or charge. This item cannot be reproduced or quoted extensively from without first obtaining permission in writing from the copyright holder(s). The content must not be changed in any way or sold commercially in any format or medium without the formal permission of the copyright holders.

This document is the author's post-print version, incorporating any revisions agreed during the peer-review process. Some differences between the published version and this version may remain and you are advised to consult the published version if you wish to cite from it.

1 Exploring the effects of geotextiles in the performance of highway filter 2 drains

3 L.A. Sañudo-Fontaneda ^{1*}, S.J. Coupe ², S.M. Charlesworth ³, E.G.Rowlands ⁴

4 ¹ Department of Construction and Manufacturing Engineering. University of Oviedo. Polytechnic School
5 of Mieres. Calle Gonzalo Gutierrez Quiros s/n. 33600, Mieres (Asturias), Spain. Email:
6 sanudoluis@uniovi.es

7 ² Centre for Agroecology, Water and Resilience (CAWR), Coventry University, Ryton Gardens, Wolston
8 Lane, Ryton-on-Dunsmore, CV8 3LG, Coventry, UK. Email: steve.coupe@coventry.ac.uk

9 ³ Centre for Agroecology, Water and Resilience (CAWR), Coventry University, Ryton Gardens, Wolston
10 Lane, Ryton-on-Dunsmore, CV8 3LG, Coventry, UK. Email: sue.charlesworth@coventry.ac.uk

11 ⁴ Carnell Group Ltd. Gothic House, Market Place, ST19 5DJ, Penkridge, United Kingdom. Email:
12 gordon.rowlands@carnellcontractors.com

13
14 *Corresponding author details: Email: sanudoluis@uniovi.es

16 Abstract

17 Highway Filter Drains (HFD) are one of the most utilised drainage systems for roads, being considered as
18 an environmental solution for sustainable drainage in transport infrastructures. However, little research
19 has been done to understand their performance, representing a significant knowledge gap. This article
20 therefore determines the hydraulic and clogging response of 3 different HFD designs in the laboratory;
21 one standard design with British Standard Type B aggregate, and 2 new designs including a geotextile
22 located at 50 mm and 500 mm depth from the surface of the HFD structure in order to assess the effect of
23 the geotextile. The laboratory models were initially subjected to 9 rainfall scenarios with 3 rainfall
24 intensities (2.5, 5 and 10 mm/h) and 3 storm durations (5, 10 and 15 minutes). Subsequently, the
25 equivalent of 2-years' worth of pollutants were added to test possible clogging issues under the highest
26 intensity rainfall event, corresponding to a 1 in 1 year return period for the West Midlands, UK. No
27 clogging issues were found in any of the models although the majority of the sediments were
28 concentrated in the first 50 mm of the HFD profile, with higher percentages (>90% of the sediment

29 added) in those models with an upper geotextile. Location of the geotextile significantly influenced (p-
30 value = 0.05) the hydraulic performance of the HFD.

31

32 **Keywords:** Geosynthetics; Clogging; Geotextile; Highway Filter Drains; Road Safety; Sustainable
33 Drainage Systems (SuDS).

34

35

36 **1. Introduction**

37 Vehicle traffic in the UK has increased dramatically since the 1950s to more than 300 billion vehicle
38 miles in 2014 (UK Department of Transport, 2015). To cope with this high volume of traffic, the UK has
39 a road network of nearly 1.8 km road/km² of land area with a total length of 419,596 km, of which 3,674
40 km are motorways and 49,040 km are main roads (Nicodeme et al. 2013).

41 The Strategic Road Network (SRN) (including motorways and A roads) (UK Department for Transport,
42 2012) and local road networks are England's most valuable infrastructure asset, valued at approximately
43 £344 billion and as well as the roads, includes other infrastructure such as bridges, embankments and
44 drainage systems (House of Commons, 2014). In 2012-2013 public spending on maintaining England's
45 roads was £4 billion, divided between the UK Department of Transport, the Highways Agency
46 (Highways England since 2015) and Local Authorities. The operation, maintenance and improvement of
47 the SRN, which represents 2% of the total road network (7,080 km), is the responsibility of The
48 Department of Transport through Highways England (House of Commons, 2014).

49 Road drainage systems are therefore a vital asset in transport infrastructure, contributing to the safety of
50 road users by removing surface runoff, improving visibility and mitigating environmental problems to
51 receiving waters. Hence, they are an important part of the maintenance programme developed by
52 Highways England (Ellis and Rowlands, 2007; Coupe et al. 2015).

53 Filter Drains (FD), kerbs and gullies connected to pipes below ground and surface water channels along
54 the pavement edge, are the main methods of dealing with surface runoff (DMRB-UK, 1997a). FD, also
55 known as 'French Drains', are not only one of the most used drainage systems in the UK, but are also an
56 historically important engineering technique across the world. FDs when used on highways are defined as
57 Highway FD or HFD, terminology which will be used hereinafter. Approximately 50% of the SRN in

58 England (in total about 7,000 km accounting for traffic flow in both directions) uses HFD as their main
59 drainage technique (Coupe et al. 2015).

60 HFD are designed to cope with a wide range of storm events, to avoid flooding problems. Thus, the
61 Design Manual for Roads and Bridges (DMRB-UK, 2004), Volume 4 Section 2 (Drainage), stipulates
62 that highway drainage systems should be designed for high intensity events over a few minutes (short
63 durations) with return periods of 1 year (with no surcharge of piped systems or road-edge channels) or 5
64 years with no flooding on the carriageway.

65 According to DMRB-UK, 1997b, UK HFDs should be a minimum of 0.6 m below the pavement sub-base
66 in order to prevent groundwater entering the pavement structure. Including the full depth of the road
67 structure, the typical depth for an HFD is up to 1 m with a width of approximately 1 m (Figure 1).

68 A perforated pipe is located at a depth of 850 mm in a full-sized HFD, details and recommendations such
69 as its diameter, the type of aggregate used for the bedding layer and the main body of the HFD are all
70 given in the Design Manual for Roads and Bridges (DMRB-UK, 2001) and the UK Highways Agency
71 Manual of Contract Documents for Highway Works (MCDH) (2009).

72 After a long operational life, often 30 to 40 years of service, some HFD may need maintenance and in
73 order to judge this, their performance is monitored using high-speed non-intrusive Ground Penetrating
74 Radar (GPR) surveys, specifically SMARTscan both on verges and central reservations (Carnell, 2015).

75 However, there is a lack of comprehensive understanding of the hydraulic processes that take place in
76 HFDs and how resistant and resilient they are to flooding and clogging.

77 The impact of this research is wider than just the UK as HFD are used in other countries across the world
78 such as the Republic of Ireland where a visual inspection carried by Bruen et al. (2006) on the Irish dual
79 carriageways and motorways found that more than 40% of them had HFD as their main drainage system.

80 Also in Ireland, issues around clogging have been commonly addressed by the use of a geotextile as a
81 barrier to fine material ingress (Bruen et al. 2006; Desta et al. 2007) whilst still allowing water to flow
82 through and into the drainage material and pipe. Other international drainage techniques similar to HFD
83 also use geotextiles such as the so-called “edge drains” in the U.S.A (Kearns, 1992; Koerner et al., 1996)
84 and Canada (Raymond et al. 2000); and also in Spain (Castro-Fresno et al. 2013; Andres-Valeri et al.
85 2014; Sañudo Fontaneda et al. 2016) where there are specifications including the use of geosynthetic
86 products in drainage structures (AENOR, 2001; Bustos et al. 2007).

87 Despite the fact that geosynthetics have been included successfully in the structure of other SuDS such as
88 Permeable Pavement Systems (PPS) in the UK (e.g. Pratt et al. 1999), their utilisation in association with
89 HFDs is still viewed with scepticism by some engineers due to concerns over possible blockage of the
90 aggregate layer and/or the pipe, leading to a reduction in infiltration capacity. In order to address these
91 issues, there were 2 aims of this research:

- 92 1. To determine the effects on HFD hydraulic performance of the inclusion of geotextiles due to its
93 water retention characteristic (WRC). This concept is described by Chinkulkijniwat et al. (2017),
94 who also highlight the lack of knowledge of geotextile WRC.
- 95 2. To determine the influence of the geotextile on the potential for clogging for short return
96 periods.

97

98 **2. Materials and Methods**

99 2.1. Experimental preparation and materials

100 Ten plate-glass rigs were set up: 4 replicates of the Standard HFD, and three replicates for each HFD
101 model containing geotextiles at 2 different depths in the profile (50 mm and 500 mm respectively). The
102 rigs had 5 mm thick walls and measured 215 mm x 215 mm x 650 mm, thus their volume was 0.030 m³
103 and surface area was 0.046 m² (see Figure 2). No lower pipe was used, since the aim was to analyse the
104 hydraulic and clogging performance of the aggregate and to isolate the influence of the geotextile layer on
105 the general performance of the HFD, following the preparation method presented in Sañudo-Fontaneda et
106 al. (2017). The outflow, used to build the hydrographs of performance for every HFD model, was
107 measured using funnels placed at the bottom of each plate-glass rig to direct the outflow to a sample
108 collector (see Figure 2).

109 The details of the materials used to replicate the three different HFD designs, as shown in Figure 2, are
110 presented below:

- 111 1. Standard HFD. Made of Type B aggregate (see Figure 2).
- 112 2. HFD + Lower Geotextile. As in the Standard HFD plus a geotextile layer at 500 mm depth from
113 the HFD surface and 50 mm from the base (see Figure 3).
- 114 3. HFD + Upper Geotextile. As in the Standard HFD above plus a geotextile layer at 50 mm depth
115 from the surface (see Figure 3).

116 The aggregate utilised in this study was that normally used in UK HFD installations and was 20-40 mm,
117 G_c 85/20, clean Granodiorite Type B. A type B aggregate Particle Size Distribution (PSD) is presented in
118 Figure 2, complying with MCDH, 2009 and BS EN 13242 requirements (BSI, 2006).

119 The geotextile was a nonwoven fabric of virgin polypropylene fibres, with an approximate mass per unit
120 area of 0.13 Kg/m². Nonwoven geotextiles have been widely used in roadworks and drainage due to their
121 supporting ability and improvement to the internal drainage of the aggregate layers (Sañudo Fontaneda et
122 al. 2016; Broda et al. 2017; Portelinha and Zornberg, 2017). This geotextile has been used previously in
123 research for example the TRAMMEL drainage system (Clapham, 1981; Ingold, 1994). It is also one of
124 the most widely used geosynthetics in Sustainable Drainage Systems (SuDS), especially PPS because of
125 its well-known pollutant removal efficiency in providing a suitable surface for trapping oil and allowing
126 microorganisms to grow (Newman et al. 2002; Coupe et al. 2003; Gomez-Ullate et al. 2010; Sañudo-
127 Fontaneda et al. 2014b). The hydraulic properties of the geotextile are given in Table 1.

128 This geotextile was also selected for its mechanical properties in terms of structural performance as it was
129 to be used at different depths in the HFD test rigs, and would therefore be subjected to different forces
130 (Table 2). The pressure generated by the weight of the aggregates perpendicular to the surface of the
131 geotextile would be 8.5 Pa in the case of a geotextile placed at 50 mm depth of the full scale HFD, and 85
132 Pa at 500 mm depth, with a bulk density of 1.7 t/m³.

133 A rainfall/runoff simulator was specifically designed and built for the project (see Figure 3) and had the
134 following characteristics:

- 135 • Intensity range for direct rainfall: 50-400 mm/h.
- 136 • Surface: 0.0441 m² (0.21 m x 0.21 m).
- 137 • Number of drippers: 9 (3 per row, total of 3 rows)
- 138 • Drop diameter: 3.5 mm.

139 Flow was controlled in real time with a flowmeter on the water delivery pipe (see Figure 3), which
140 controlled rainfall intensity to between 50-400 mm/h as required.

141

142 2.2. Experimental methodology

143 There were 2 main stages:

144 Stage 1. Hydraulic characterization of HFD performance was carried out by simulating flow produced by
145 three rainfall intensities (2.5, 5 and 10 mm/h) raining over a draining area consisting of 2 carriageways
146 and a hard-shoulder (Table 3) and three storm durations (5, 10 and 15 minutes), resulting in 9 different
147 storm scenarios. The 1 in 1 year storm required for design of HFD by the DRMB (2004) was the highest
148 rainfall event simulated at this stage 1 (10 mm/h) and the longest storm duration (15 minutes). A total of
149 90 tests were carried out, 10 runs of each storm scenario, producing a total of 2,026 infiltration rate data
150 points (outflow measured per minute on each rig and each test). The Rational Method is suggested for
151 SuDS (Woods Ballard et al. 2015), therefore calculations were undertaken to determine the relationship
152 between rainfall intensities and the flow entering the models as a result of the surface runoff produced by
153 these storm events. Two and 3 carriageways are the most common number of lanes used on UK roads;
154 this was the justification for their use in calculating runoff flows (DMRB-UK, 1999).

155 Basing the calculations on the Rational Method, laboratory rainfall events of 100, 200 and 400 mm/h
156 (intensity values which will be used hereinafter for the analysis of the laboratory results) controlled by the
157 flowmeter connected to the rainfall/runoff simulator (see Figure 3) were generated over the surface of the
158 laboratory models (0.046 m² surface area) in order to accomplish the rainfall scenarios and runoff flows
159 represented on Table 3.

160 Stage 2. Pollutants were periodically added to the rigs once Stage 1 was completed in order to simulate 2
161 years in-use of the HFD models, each rig was therefore subjected to the following conditions in terms of
162 pollutant addition:

- 163 ○ Amount of sediment: 30 g/rig/test (i.e. 360 g added to each rig in total over the course of the
164 experiments) just before the addition of oil, representing sediment deposited on West Midland, UK
165 highways of approximately 1,000 kg/m/year (Carnell Group Ltd., *pers comm*). The sediment was
166 obtained from arisings collected from gully pots connected to HFD pipes from a highway in the West
167 Midlands, UK. For each rig, 12 rainfall events of 10 mm/h raining over a drainage area consisting of
168 2 carriageways and a hard-shoulder of 15 minutes' duration (replicating the worst case scenario); a
169 total of 120 tests were carried out, producing a total of 2,739 infiltration measurements (outflow
170 measured per minute for each test). The intensity and storm duration used represented a 1 in 1-year
171 storm event in the West Midlands (UK) (Sañudo-Fontaneda et al. 2016), as required to avoid
172 surcharge in the pipe by the DMRB-UK 2004. The West Midlands was used as the reference for

173 calculations, both from the amount of sediments and the rainfall volumes, due to the fact that there
174 will be field studies undertaken in the future which will use the laboratory studies as comparators.
175 The reason for using 2 years' worth of sediments was based on previous studies carried out by
176 Mitchell (2015) in Scotland which indicated 2 years until the start of clogging issues, both in the
177 surface layer and the pipe at the bottom of the HFD.

178 ○ Amount of oil: 6.121 g/rig/test (74.58 g of oil was added to each rig in total over the course of the
179 experiments) was based on Gomez-Ullate et al. (2010), Sañudo-Fontaneda et al. (2014b) and Bayon
180 et al. (2015) who multiplied the suggested 9.27 g/year/m² by Pratt et al. (1999) by 100 to represent a
181 worst-case scenario such as a catastrophic oil spill from a car sump. The oil was a used part synthetic
182 lubricating oil, mainly composed of high molecular weight fractions, with C21-C40 making up
183 99.03% of total petroleum hydrocarbons (TPH).

184 2.3. Experimental analyses

185 The effect of the inclusion of a geotextile layer on HFD performance was investigated using 2 main
186 approaches:

- 187 • Hydraulic performance of the HFD designs
- 188 ○ Hydrographs of performance. The hydrographs were plotted at minute intervals using the volume of
189 outflow measured in the sample collectors (Figure 3) from each rig under the different rainfall
190 scenarios and then comparing the influence of the addition or not of geotextiles and pollutants. The
191 outflow represented the infiltration rate for the whole HFD system simulated in the laboratory.
- 192 • Attenuation performance. Attenuation is considered to be the retention of rainfall in the HFD
193 structure before production of the first outflow discharge during a storm event since the beginning of
194 the rainfall event simulated. This could be affected by the presence or absence of a geotextile and
195 hence was used to provide an indication of HFD performance. This time represented the capacity of
196 each HFD design to delay commencement of discharge flow, and also the time to reach peak-flow.
- 197 • Geotextile effect on the hydraulic and clogging performance of HFD. Once the hydraulic
198 performance of HFD was analysed, the effect of the inclusion of a geotextile in the HFD structure
199 was analysed in isolation, including the study of potential clogging scenarios derived from the
200 presence of the geotextile, as it is shown below:

201 ○ Geotextile effect on the hydraulic performance of HFD. Statistical analyses were carried out in order
202 to assess the influence of the geotextile on the attenuation levels used to measure the hydraulic
203 performance in the HFD designs.

204 ○ Geotextile effect on the potential for clogging on HFD. The accumulation of pollutants at different
205 levels within the HFD structure measured from the surface was analysed in order to determine where
206 the sediments preferentially deposited within the HFD structure. Once all the hydraulic experiments
207 were finished, the sediments were carefully recovered from the laboratory models and weighed. The
208 trapping efficiency of each HFD design was measured by weighing the sediments accumulated in the
209 whole model profile at the end of all experiments and comparing them with the amount of sediments
210 added to the rigs.

211

212 **3. Results and Discussions**

213 3.1. Hydraulic performance of the HFD designs (hydrographs and attenuation levels)

214 3.1.1. Stage 1: Hydraulic performance of the HFD test rigs

215 Hydrographs of performance were produced for all storm durations (5, 10 and 15 minutes), including all
216 HFD designs (no geotextile, lower geotextile and upper geotextile) and laboratory rainfall intensities
217 (100, 200 and 400 mm/h). Figures 4, 5 and 6 show hydrographs for the 5-minute storm duration only as
218 the trends for 10 and 15 minutes were similar.

219 Figures 5 and 6 show that, at the higher rainfall intensities (200 and 400 mm/h) the test rigs behaved in a
220 similar manner. However, at 100 mm/h (Figure 4) there was more of a discrepancy between the rigs;
221 those with an upper geotextile in particular exhibiting lower rates than the others, as well as longer delays
222 in both the rising and falling limbs. Effluent took approximately 60 secs to be recorded after rainfall for
223 the higher rainfall intensities, but did not appear until 102 seconds in the rigs rained on at 100 mm/h. As
224 intensity increased, the time to base flow reduced, and again at 100 mm/h those rigs with the upper
225 geotextile took longer than any of the other rigs regardless of structure or rainfall intensity.

226 Regardless of rig structure, Figure 7 shows that at the lower rainfall intensities peak flow was achieved at
227 the same time, approximately 300 seconds. However, for the higher rainfall intensities, the structures
228 behaved slightly differently, with all 3 taking less time to peak than at lower intensities. Those with no

229 geotextile reached the peak more quickly than those with a lower geotextile which were quicker than rigs
230 with an upper geotextile.

231 In order to assess the statistical significance of geotextile location, duration of the simulated rainfall and
232 its intensity, statistical testing was undertaken. A Kolmogorov-Smirnov test was carried out in order to
233 check whether the data were normally distributed. The potential influence of the presence of a geotextile
234 on hydraulic performance was analysed using ANOVA for parametric variables (normally distributed)
235 with k-samples (3 for geotextile location: no geotextile, lower geotextile and upper geotextile). ANOVA
236 was also used to check the statistical significance of storm duration on attenuation, and the influence of
237 rainfall intensity on attenuation performance was tested using Kruskal Wallis. Table 4 summarises the
238 results of these statistical tests, showing that geotextile location had a significant influence on attenuation,
239 as did rainfall intensity, both at the 95% confidence level. However, storm duration was found not to
240 significantly affect attenuation performance.

241 Table 5 shows the impact of rig structure and rainfall intensity on attenuation performance through the
242 use of equations of performance (trends). The values of R^2 for the rigs without a geotextile and those
243 including a lower geotextile were >0.70 , whilst that for the rigs with an upper geotextile was >0.5 .

244

245 3.1.2. Stage 2: the effect of pollutant addition on HFD performance

246 That the addition of pollutants did influence hydraulic performance is illustrated in Figure 8 which shows
247 that the capacity of the system was reduced in terms of its ability to attenuate the storm peak. Sediments
248 also introduced higher variability as it can be seen in the number of outlayers within the experiments.
249 This particular behaviour from the sediments was highlighted by Sañudo-Fontaneda et al. (2013) when
250 studying the reduction of the infiltration capacity of PPS under different clogging scenarios.

251 It was also found that geotextile position influenced hydraulic performance (Figure 9) since the time to
252 peak for all models was increased from no geotextile structures to an upper geotextile. This finding
253 suggests that designers and practitioners looking for an increase in the time to peak should include the
254 geotextile closer to the surface of the HFD.

255

256 3.2 Geotextile effect on the hydraulic and clogging performance of HFD

257 3.2.1 Geotextile effect on the hydraulic performance of HFD

258 Initial bivariate correlation analyses shown in Table 6 highlighted significant linear relationships between
259 attenuation performance and the addition of sediments at a 95% confidence level as well as high
260 correlation between attenuation, rainfall intensity, storm duration and geotextile location.

261 In order to confirm these preliminary findings, a Kruskal Wallis test was carried out to compare the
262 influence of the inclusion of a geotextile on hydraulic performance using attenuation levels, whilst a
263 Mann-Whitney test was performed to validate the influence of sediment addition on hydraulic
264 performance. The results are shown in Table 7 which confirmed that the addition of sediments and the
265 presence of a geotextile had a statistically significant effect on hydraulic performance.

266

267 3.2.2 The presence of a geotextile and its effect on the potential for clogging

268 No clogging issues were observed during storm events that simulated 2-years' worth of pollutant addition
269 (sediments and oil) over the laboratory models although the hydraulic behaviour was found to be
270 different.

271 Eventually, however, a crust of oil and sediment developed on the rig surface and began to create an
272 impermeable layer preventing the downprofile migration of the sediment as found in other studies such as
273 Mitchell (2015).

274 It was found that the pollutants preferentially accumulated in the top 50 mm of the HFD profile despite
275 the presence of geotextile as can be seen in Table 8. More than 70% of the total amount of pollutants
276 added to the models were found in the top of the profile for rigs either without a geotextile, or with one
277 located lower in the profile. However, 98.2% of the pollutants were found at the top of the profile for rigs
278 with an upper geotextile. Whilst complete clogging of the system was not an issue over the course of the
279 experiments, nonetheless the likelihood would be that the rigs with an upper geotextile would eventually
280 clog, and more quickly than the other structures being tested. In fact, Zhao et al. (2016) found that
281 nonwoven geotextiles are beneficial in providing a groundwater drainage layer. However, there are other
282 possible variables influencing the loss of hydraulic capacity in the field such as chemical clogging
283 (Veylon et al. 2016).

284 Based on this study, the hydraulic deterioration of geosynthetics should be addressed in long-term field
285 studies in order to quantify the potential for clogging when used in an HFD. Furthermore, Yoo (2016)

286 pointed out the need to understand the hydraulic deterioration of geosynthetic filter drainage systems for
287 their use in other civil engineering structures such as tunnels.

288

289 **4. Conclusions**

290 This research has shown that using a geotextile in an HFD can contribute positively to improve the safety
291 of highways since peak flow is delayed as is time to peak due to the geotextile's ability to become wet
292 whilst maintaining a head of water before allowing it to pass through (WRC).

293 Increasing rainfall intensity influenced the hydraulic performance of HFD rigs by decreasing time to peak
294 in all designs. However, storm duration did not influence peak attenuation in any of the HFD designs,
295 although it did affect the volume of runoff infiltrated. In addition, the presence of a geotextile influenced
296 hydraulic performance by increasing peak attenuation, hence delaying the time to peak in comparison
297 with rigs without a geotextile. Moreover, the position of the geotextile layer influenced hydraulic
298 performance (p -value = 0.05), with the higher geotextile exhibiting longer times to peak, followed by the
299 lower geotextile; rigs without a geotextile had the shortest time to peak.

300 The addition of pollutants (sediments and oil) significantly influenced hydraulic performance of all
301 designs, reducing the capacity for infiltration with the eventual formation of an impermeable crust at the
302 surface of the rigs. The majority of applied pollutants preferentially accumulated higher in the HFD
303 profile in the top 50 mm, confirming the findings of previous studies such as Mitchell (2015) and Coupe
304 et al. (2015). Furthermore, the presence of an upper geotextile trapped more than 95% of the applied
305 pollutants in the top 50 mm of the profile in comparison with the lower geotextile (75.9%) and no
306 geotextile (72.4%). Finally, no clogging was observed as a result of the addition of 2 years' worth of
307 sediment.

308

309 **Acknowledgements:**

310 The authors would like to thank Carnell Support Services Ltd for funding the study. Luis A. Sañudo-
311 Fontaneda also wish to thank the funding for the development of the UOStormwater Engineering
312 Research Team by the University of Oviedo through the research project with reference PAPI-17-
313 PEMERG-22.

314

315 **References**

- 316 AENOR, 2001. UNE-EN 13252:2001. Geotextiles and geotextile-related products. Characteristics
317 required for use in drainage systems.
- 318 Andrés-Valeri, V.C.A., Castro-Fresno, D., Sañudo-Fontaneda, L.A., and Rodriguez-Hernandez, J., 2014.
319 ‘Comparative analysis of the outflow water quality of two sustainable linear drainage systems’.
320 *Water Science and Technology*, 70 (8), 1341-1347.
- 321 Bayon, J.R., Jato-Espino, D., Blanco-Fernandez, E., Castro-Fresno, D., 2015. Behaviour of geotextiles
322 designed for pervious pavements as a support for biofilm development. *Geotextiles and*
323 *Geomembranes*, 43 (2), 139-147.
- 324 British Standards Institution (BSI), 2006. BS EN 13242: Aggregates for unbound and hydraulically
325 bound materials for use in civil engineering work and road construction. London: BSI.
- 326 Broda, J., Gawlowski, A., Laszczak, R., Mitka, A., Przybylo, S., Grzybowska-Pietras, J., Rom, M., 2017.
327 Application of innovative meandricly arranged geotextiles for the protection of drainage ditches in
328 the clay ground. *Geotextiles and Geomembranes*, 45 (1), 45-53.
- 329 Bruen, M., Johnston, P., Quinn, M.K., Desta, M., Higgins, N., Bradley, C., and Burns, S., 2006. “Impact
330 Assessment of Highway Drainage on Surface Water Quality”. Report prepared for the
331 Environmental protection Agency by the Centre for Water Resources Research, University College
332 Dublin.
- 333 Bustos, G. and Pérez, E., 2007. Pliego de prescripciones técnicas generales para obras de carreteras y
334 puentes. 5th Edition. Ediciones LITEAM. Madrid, Spain.
- 335 Carnell, 2015. SMARTscan. <http://www.carnellgroup.co.uk/Services/Drainage2/SMARTscan/>
- 336 Castro-Fresno, D., Andrés-Valeri, V.C., Sañudo-Fontaneda, L.A., and Rodriguez-Hernandez, J., 2013.
337 ‘Sustainable drainage practices in Spain, specially focused on pervious pavements.’ *Water*, 5 (1),
338 67-93.
- 339 Chinkulkijniwat, A., Horpibulsuk, S., Bui Van, D., Udomchai, A., Goodary, R., Arulrajah, A., 2017.
340 Influential factors affecting drainage design considerations for mechanical stabilised earth walls
341 using geocomposites. *Geosynthetics International*, 24 (3), 224-241.
- 342 Clapham, H.G., 1981. The TRAMMEL Drainage System. Transport Research Laboratory. American
343 Society of Civil Engineers (ASCE). 24-26 pp.

344 Coupe, S.J., Smith, H.G., Newman, A.P., Puehmeier, T., 2003. Biodegradation and microbial diversity
345 within permeable pavements. *European Journal of Protistology*, 39 (4), 495-498.

346 Coupe, S. J., Sañudo-Fontaneda, L. A., Charlesworth, S. M., Rowlands, E. G. Research on novel highway
347 filter drain designs for the protection of downstream environments. SUDSnet International
348 Conference, Coventry, UK, 2015. Available from:
349 <http://sudsnet.abertay.ac.uk/SUDSnetConf2015.htm>.

350 Coupe, S.J., Sañudo-Fontaneda, L.A., McLaughlin, A-M., Charlesworth, S.M., Rowlands, E.G. The
351 retention and in-situ treatment of contaminated sediments in laboratory highway filter drain models.
352 Water Efficiency Network Conference (WATEFCON 2016). *Water Frontiers: Strategies for 2020*
353 and beyond. Coventry, UK, September 2016. Available from:
354 http://www.watefnetwork.co.uk/files/default/resources/Conference2016/Session_One/45-
355 [COUPE.pdf](#).

356 Desta, M.B., Bruen, M., Higgins, N., and Johnston, P., 2007. Highway runoff quality in Ireland. *Journal*
357 *of Environmental Monitoring*, 9, 366-371.

358 DMRB-UK, 1996. Design Manual for Roads and Bridges: Geotechnics and Drainage. Vol. 4, sec. 2, part
359 3. (HD 33/96). SURFACE AND SUB-SURFACE DRAINAGE SYSTEMS FOR HIGHWAYS.
360 Technical Report, Highways Agency, UK.

361 DMRB-UK, 1997a. Design Manual for Roads and Bridges: Geotechnics and Drainage. Vol. 4, sec. 2, part
362 4. (HA 37/97). Hydraulic design of road-edge surface water channels. Technical Report, Highways
363 Agency, UK.

364 DMRB-UK, 1997b. Design Manual for Roads and Bridges: Geotechnics and Drainage. Vol. 4, sec. 2, part
365 4. (HA 79/97). Edge of pavement details for porous asphalt surface courses. Technical Report,
366 Highways Agency, UK.

367 DMRB-UK, 1999. Design Manual for Roads and Bridges: Traffic Capacity of Urban Roads. Vol. 5, sec.
368 1, part 3. (TA 79/99 Amendment No 1).

369 DMRB-UK, 2001. Design Manual for Roads and Bridges: Geotechnics and Drainage. Vol. 4, sec. 2, part
370 5. (HA 40/01). Determination of pipe and bedding combinations for drainage works. Technical
371 Report, Highways Agency, UK.

372 DMRB-UK, 2004. Design Manual for Roads and Bridges: Geotechnics and Drainage. Vol. 4, sec. 2, part
373 1. (HA 106/04). Drainage of runoff from natural catchments. Technical Report, Highways Agency,
374 UK.

375 Ellis, J.B., Rowlands, E.G., 2007. Highway filter drain waste arisings: A challenge for urban source
376 control management? *Water Science and Technology*, 56 (10), 125-131.

377 Gomez-Ullate, E., Bayon, J.R., Coupe, S., Castro-Fresno, D., 2010. Performance of pervious pavement
378 parking bays storing rainwater in the north of Spain. *Water Science and Technology*, 62(3), 615-
379 621.

380 House of Commons, 2014. Maintaining strategic infrastructure: roads. Fifteenth Report on Session 2014-
381 2015. Committee of Public Accounts. London: The Stationery Office Limited.
382 <http://www.publications.parliament.uk/pa/cm201415/cmselect/cmpubacc/105/105.pdf>.

383 Ingold, T.S., 1994. Prefabricated fin drains and their application. *Geotextiles and Geomembranes:*
384 *Manual*. Elsevier Advance Technology, UK.

385 Kearns, R.E., 1992. Long-term performance of geocomposites used as highway edge drains. *Geotextiles*
386 *and Geomembranes*, 11(4-6), 513-521.

387 Koerner, G.R., Koerner, R.M., Wilson-Fahmy, R.F., 1996. Field performance of geosynthetic highway
388 drainage systems. *ASTM Special Technical Publication*, 1281, 165-180.

389 MCDH, 2009. *Manual of Contract Documents for Highway Works. Volume 1 - Specification for*
390 *Highway Works. Series 500: Drainage and Service Ducts*. Highways Agency, UK.

391 Mitchell, G., 2015. Clogging of filtration SUDS. Long term performance of trunk road filter drains.
392 SUDSnet International Conference, Coventry, UK, 2015. Available from:
393 http://sudsnet.abertay.ac.uk/documents/SUDSnet2015_Mitchell_CloggingofFiltrationSuDS.pdf.

394 Newman, A.P., Pratt, C.J., Coupe, S.J., Cresswell, N., 2002. Oil bio-degradation in permeable pavements
395 by microbial communities. *Water Science and Technology*, 45(7), 51-56.

396 Nicodeme, C., Diamandouros, K., Diez, J., Durso, C., Brex, C., Metushi, S., 2013. European Union
397 Road Federation. *European Road Statistics 2012. Report*.
398 http://www.irfnet.eu/images/Statistics/ER_Statistics_Final_2012.pdf.

399 Portelinha, F.H.M., Zornberg, J.G., 2017. Effect of infiltration on the performance of an unsaturated
400 geotextile-reinforced soil wall. *Geotextiles and Geomembranes*, 45(3), 211-226.

401 Pratt, C.J., Newman, A.P., Bond, P.C., 1999. Mineral oil big-degradation within a permeable pavement:
402 Long term observations. *Water Science and Technology*, 39(2), 103-109.

403 Raymond, O.P., Bathurst, R.J., Hajek, J., 2000. Evaluation and suggested improvements to highway edge
404 drains incorporating geotextiles. *Geotextiles and Geomembranes*, 18(1), 23-45.

405 Sañudo-Fontaneda, L.A., Rodriguez-Hernandez, J., Vega-Zamanillo, A., Castro-Fresno, D., 2013.
406 Laboratory analysis of the infiltration capacity of Interlocking Concrete Block Pavements in car
407 parks. *Water Science and Technology* 2013, 67(3), 675-681.

408 Sañudo-Fontaneda, L.A., Andrés-Valeri, V.C.A., Rodriguez-Hernandez, J., and Castro-Fresno, D., 2014a.
409 Field study of the reduction of the infiltration capacity of porous mixtures surfaces tests. *Water*, 6
410 (3), 661-669.

411 Sañudo-Fontaneda, L.A., Charlesworth, S., Castro-Fresno, D., Andrés-Valeri, V.C.A., and Rodriguez-
412 Hernandez, J., 2014b. Water quality and quantity assessment of pervious pavements performance in
413 experimental car park areas. *Water Science and Technology*, 69(7), 1526-1533.

414 Sañudo Fontaneda, L.A., 2014. The analysis of rainwater infiltration into permeable pavements, with
415 concrete blocks and porous mixtures, for the source control of flooding. PhD Thesis, University of
416 Cantabria, Spain. Available from: <https://repositorio.unican.es/xmlui/handle/10902/5053>.

417 Sañudo-Fontaneda, L.A., Jato-Espino, D., Lashford, C., Coupe, S.J., 2016. Investigation of the design
418 considerations for Highway Filter Drains through the comparison of stormwater management tools
419 with laboratory simulation experiments. 9th International Conference NOVATECH. Planning &
420 Technologies for Sustainable Urban Water Management. Lyon, France.

421 Sañudo Fontaneda, L.A., Blanco-Fernández, E., Coupe, S.J., Carpio Garcia, J., Newman, A.P., Castro-
422 Fresno, D., 2016. Use of Geosynthetics for Sustainable Drainage. Book chapter in “Sustainable
423 Surface Water Management: A Handbook for SUDS” pp. 142-155. Ed. Wiley, U.S.A., ISBN: 978-
424 1-118-89770-6.

425 Sañudo-Fontaneda, L.A., Jato-Espino, D., Lashford, C., Coupe, S.J., 2017. Simulation of the hydraulic
426 performance of highway filter drains through laboratory models and stormwater management tools.
427 *Environmental Science and Pollution Research*, 1-10. Article in Press.

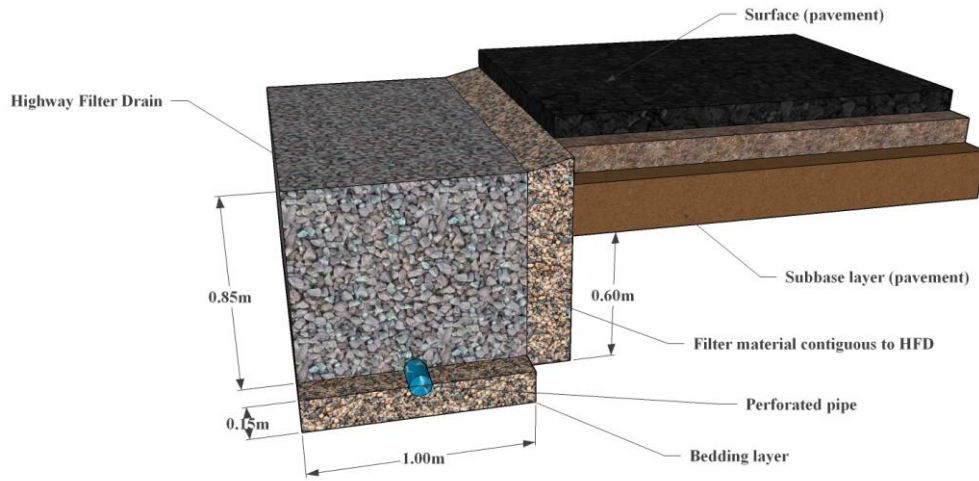
428 UK Department for Transport, 2012. Guidance on Road Classification and the Primary Route Network.
429 Available from:

430 https://www.gov.uk/government/uploads/system/uploads/attachment_data/file/315783/road-
431 [classification-guidance.pdf](https://www.gov.uk/government/uploads/system/uploads/attachment_data/file/315783/road-classification-guidance.pdf).
432 UK Department of Transports, 2015. National Road Traffic Survey.
433 <https://www.gov.uk/government/statistical-data-sets/tra01-traffic-by-road-class-and-region-miles>.
434 Veylon, G., Stoltz, G., Mériaux, P., Faure, Y.-H., Touze-Foltz, N., 2016. Performance of geotextile filters
435 after 18 years' service in drainage trenches. *Geotextiles and Geomembranes*, 44 (4), pp. 515-533.
436 Woods Ballard, B., Wilson, S., Udale-Clark, H., Illman, S., Ashley, R and Kellagher, R., 2015. The SuDS
437 manual, CIRIA 753. CIRIA. ISBN 979-0-86017-760-9.
438 Yoo, C., 2016. Hydraulic deterioration of geosynthetic filter drainage system in tunnels – its impact on
439 structural performance of tunnel linings. *Geosynthetics International*, 23(6), 463-480.
440 Zhao, A., Oelkers, C., Diviacchi, V., 2016. Geocomposite for landfill's groundwater drainage layer.
441 *Geosynthetics*, 34(1).
442

443

FIGURES

444

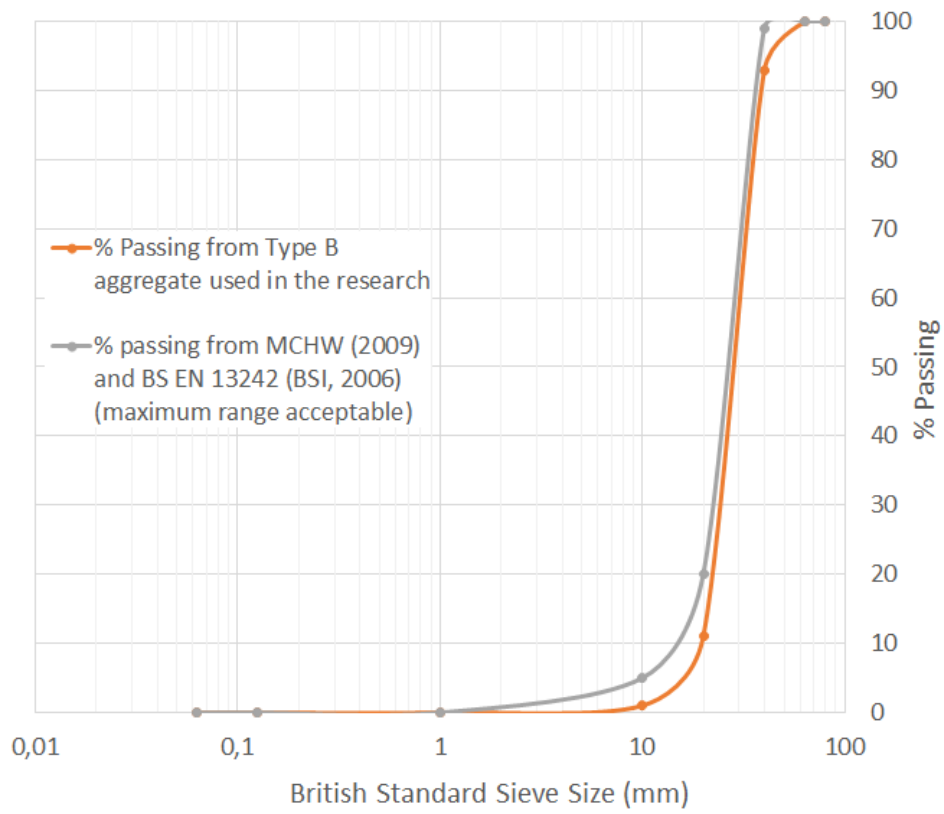


445

446

Figure 1. Standard HFD design and detail of its position relative to the edge of the highway.

447



448

449

Figure 2. Gradation curve for the Type B aggregate.

450

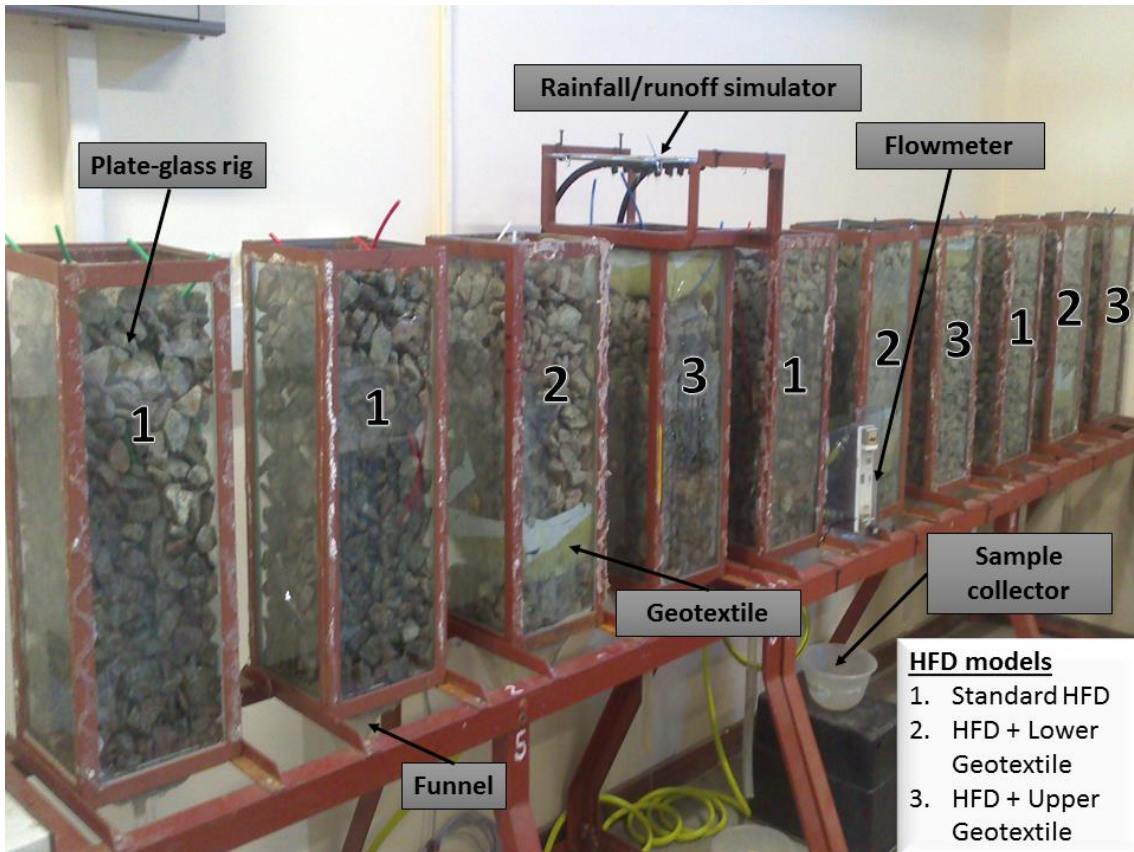
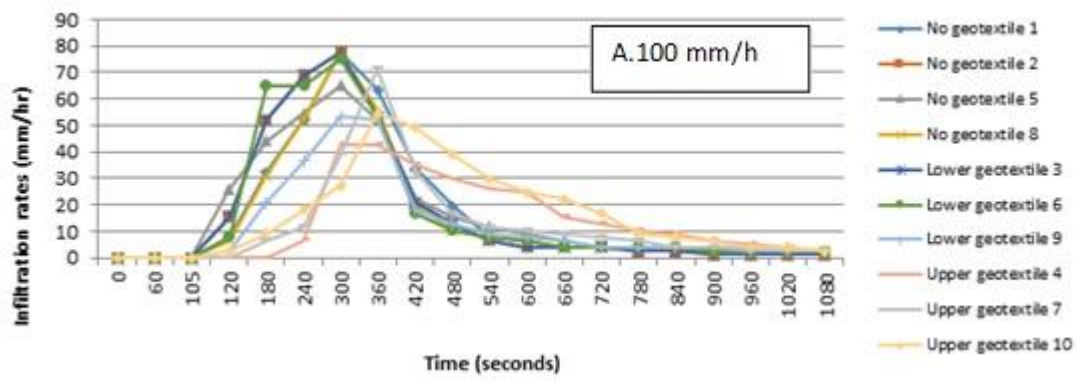


Figure 3. HFD laboratory models setup including the bespoke rainfall/runoff simulator.

451
452

453



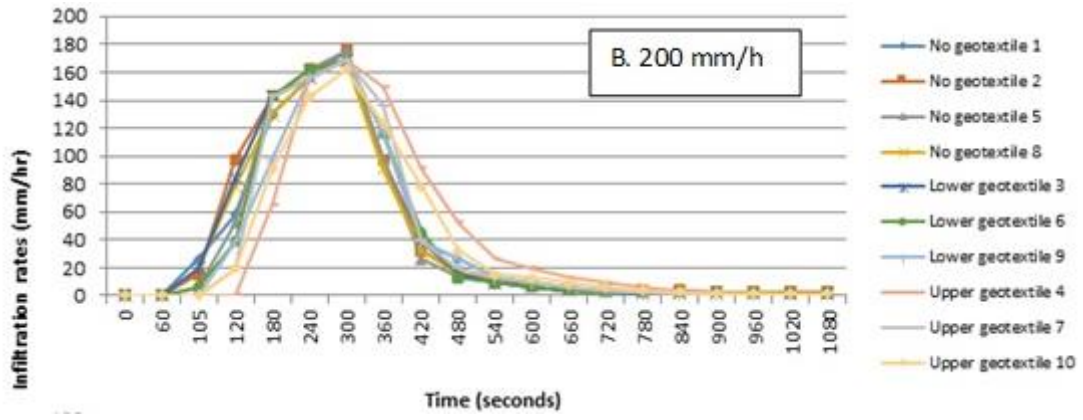
454

455

Figure 4. Hydrographs of performance of the three different designs for a storm event of 5 minutes' duration at 100

456

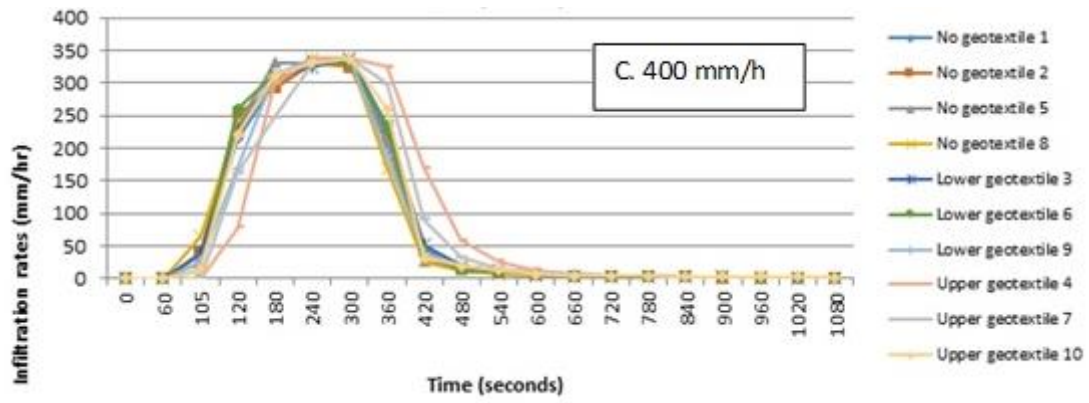
mm/h simulated rainfall intensity.



457

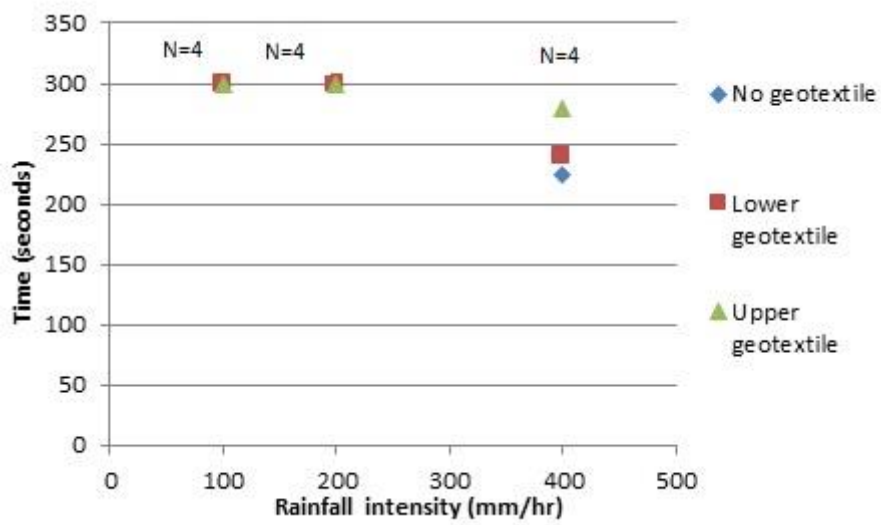
458 Figure 5. Hydrographs of performance of the three different designs for a storm event of 5 minutes' duration at 200
 459 mm/h simulated rainfall intensity.

460



461

462 Figure 6. Hydrographs of performance of the three different designs for a storm event of 5 minutes' duration at 400
 463 mm/h simulated rainfall intensity.



464

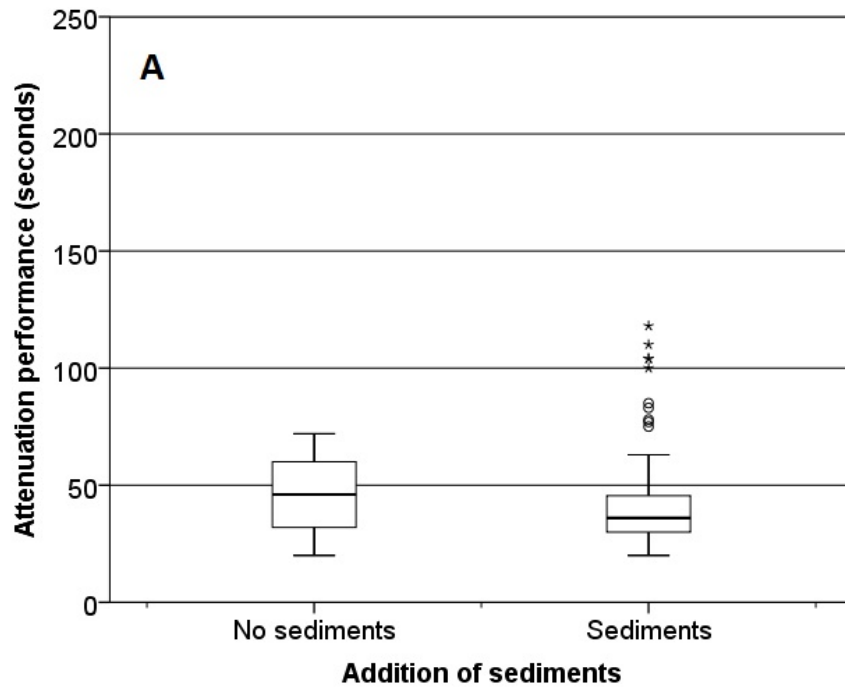
465

Figure 7. Mean time to peak from each HFD design (average of all laboratory models for each type of design)

466

measured dependent upon rainfall intensity and according to rig structure.

467

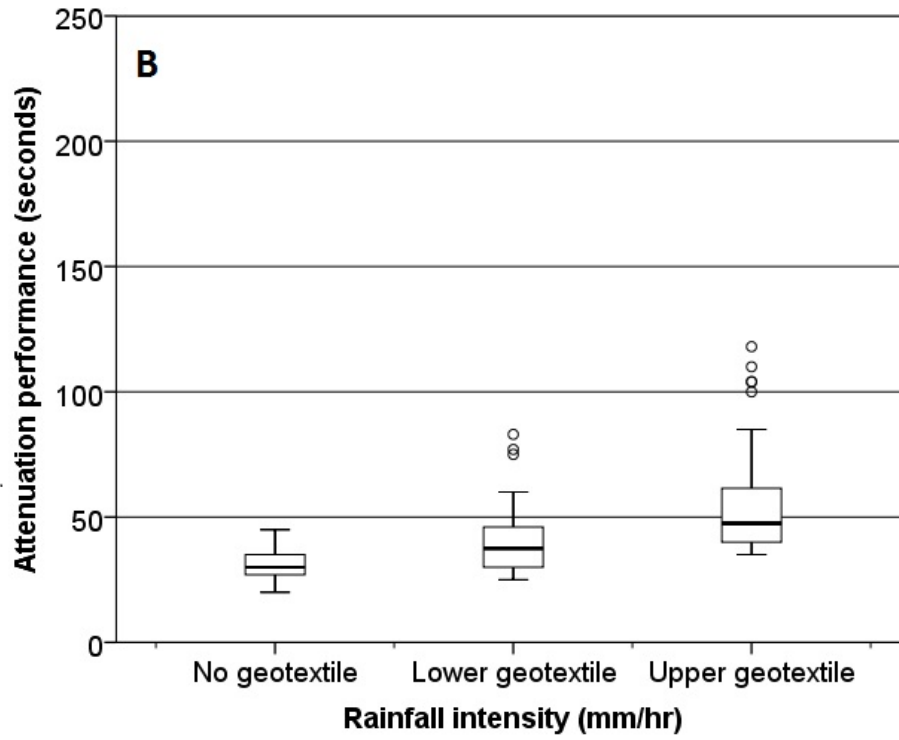


468

469

Figure 8. Box-plots comparing the effect of pollutant addition on peak attenuation.

470



471

472

Figure 9. Box-plots comparing the influence of different geotextile positions on attenuation performance.

473

474

475

TABLES

476

477

Table 1. Hydraulic properties of the geotextile.

Hydraulic property	Standard	Units	Value
Permeability (H ₅₀)	EN ISO 11058	L/m ² s	100
Opening Size (O ₉₀)	EN ISO 12956	μm	150

478

Table 2. Mechanical and physical properties of the geotextile.

Mechanical properties (mean values)	Standard	Units	T1000
Tensile Strength	EN ISO 10319	kN/m	8.0
Tensile at 5% Elongation	EN ISO 10319	kN/m	3.4
Tensile Elongation	EN ISO 10319	%	24
CBR Puncture Resistance	EN ISO 12236	N	2000
Cone Drop	EN ISO 13433	mm	34
Physical properties (mean values)	Standard	Units	T1000
Thickness at 2kPa	EN ISO 9863-1	mm	0.75

481 Table 3. Surface runoff flow per HFD linear meter produced by several rainfall intensities depending on
 482 the number of carriageways associated with the highway.

Rainfall intensity (mm/hr)	2 carriageways (6 m) + hard shoulder (1.8 m) (L/s·m)	3 carriageways (9 m) + hard shoulder (1.8 m) (L/s·m)
2.5	0.0054	0.0075
5	0.0109	0.0150
10	0.0217	0.0300

483

484 Table 4. Results of ANOVA testing the significance of geotextile location and storm duration on attenuation
 485 performance and Kruskal Wallis testing for the significance of rainfall intensity on attenuation performance.

Significance test		Attenuation performance
ANOVA	Fisher-Snedecor's F	13.091
(Geotextile location)	Significance	0.000
ANOVA	Fisher-Snedecor's F	0.378
(Storm duration)	Significance	0.686
Kruskal Wallis	Chi-square	50.264
(Grouping variable: Rainfall intensity)	Asymptotic significance	0.000

486

487

Table 5. Trends in the attenuation performance for the 3 HFD designs, depending on the rainfall intensity.

Rainfall intensity (mm/hr)	Equation	R²
No geotextile	$y = 1040,1x^{-0,559}$	0.7375
Upper geotextile	$y = 0,0014x^2 - 0,93x + 215,89$	0.5090
Lower geotextile	$y = 846,49x^{-0,492}$	0.7917

488

489 Table 6. Statistical analysis of the bivariate correlations (Spearman's Rho coefficients) between the outcome variable
 490 attenuation performance, and the variables addition of sediments, geotextile location, rainfall intensity and storm
 491 duration.

Variable		Addition of sediments	Geotextile location	Rainfall intensity	Storm duration
Attenuation performance	Correlation coefficient	- 0.507**	0.489**	- 0.628**	- 0.365**
	Significance (bilateral)	0.000	0.000	0.000	0.000

** Correlation is significant at the level of 0.01 (bilateral).

* Correlation is significant at the level of 0.05 (bilateral).

492

493 Table 7. Mann-Whitney and Kruskal Wallis statistical tests for the analysis of the significance influence of the
 494 variables addition of sediments and geotextile location on the attenuation performance.

Significance test	Attenuation performance	
Mann-Whitney*	Mann-Whitney's U	2,451.5
	Asymptotic significance (bilateral)	0.000
Kruskal Wallis**	Chi square	52.093
	Asymptotic significance	0.000

* Grouping variable: addition of sediments.

** Grouping variable: geotextile location.

495

Table 8. Cumulative percentage of sediment found at different levels in the HFD rig profiles.

% sediment found down profile in the HFD rigs	Standard HFD	Lower geotextile	Upper geotextile
Top (50 mm from the surface)	72.4	75.9	98.2
Middle (between 50 and 500 mm from the surface)	89.8	96.3	99.1
Bottom (500 mm from the surface)	100.0	100.0	100.0